

# Unraveling the Complexity of Lipidomes by Multiple Heart-Cutting Q-TOF LC/MS with the Agilent 1290 Infinity 2D-LC Solution



## Authors

Gerd Vanhoenacker<sup>1</sup>,  
Ruben t'Kindt<sup>1,2</sup>, Frank David<sup>1</sup>,  
Pat Sandra<sup>1,2</sup>, and  
Koen Sandra<sup>1,2</sup>

<sup>1</sup> Research Institute for  
Chromatography  
President Kennedypark 26  
B-8500 Kortrijk  
Belgium

<sup>2</sup> Metablys  
President Kennedypark 26  
B-8500 Kortrijk  
Belgium

Udo Huber  
Agilent Technologies, Inc.  
Waldbronn, Germany

## Abstract

The Agilent 1290 Infinity 2D-LC solution was used to study the lipid composition of blood plasma and induced sputum samples. Applying multiple heart-cutting enabled a fully automated HILIC-based lipid (sub-)class type fractionation in the first dimension and online transfer of the fractions onto a high-resolution reversed-phase UHPLC column in the second dimension for separation of group members according to hydrophobicity. Detection and identification of the lipids was carried out with the Agilent Accurate-Mass Q-TOF LC/MS System. The main advantage of this approach is a significant reduction of the number of lipids that enter the mass spectrometer at a given time. This reduces the risk of misidentification and erratic quantification in complex lipid samples due to interfering isobaric lipids or isotopes of lipids.

## Introduction

The lipidome can be described as the complete lipid content in a given sample.<sup>1</sup> Lipids exist in different classes with different physicochemical and biological properties. Each class contains many members that differ in the length of the fatty acid side-chain and the number of double bonds, among others. Lipid extracts generally are complex mixtures with a significant structural diversity and a large dynamic range. As a result, the measurement of the total lipid content is an analytical challenge and requires a high performance separation step followed by high-resolution mass spectrometry.

Several approaches are available for this type of analysis, and state-of-the-art UHPLC on high performance LC columns enables the high-resolution separation required for detailed profiling of lipids in complex biological matrixes. We have recently reported on lipidomic analyses in blood plasma<sup>2</sup> and induced sputum.<sup>3</sup> These studies have shown that a better chromatographic separation is beneficial for MS data analysis and facilitates lipid identification and quantification.

Several options are available for improving the chromatographic separation. Multidimensional chromatographic solutions are an efficient way to drastically increase peak capacity. In two-dimensional LC (2D-LC), comprehensive LCxLC is known to substantially increase the chromatographic resolution as long as the two dimensions are orthogonal and the separation obtained in the first dimension is maintained upon transfer to the second dimension.<sup>4</sup> In the comprehensive LCxLC mode, each fraction collected from the first dimension column is transferred to a second dimension separation for

analysis. A less complex approach in 2D-LC is heart-cutting (LC-LC), where only one or a few fractions are transferred to the second dimension. The advantage of this multidimensional mode is that the second dimension analysis time is not limited by the 2D-LC modulation time. Therefore, a better separation of the transferred fractions can be achieved.

The application of 2D-LC for complex lipid samples is not new, and several column combinations have been reported. The most obvious combinations are a normal phase or HILIC separation in the first dimension and a reversed-phase (RPLC) mechanism in the second dimension. Such combinations have proven to result in good orthogonality for lipid samples. The first dimension provides a separation based on the polar head-group of the lipids, resulting in a lipid (sub-)class separation (for example, phospholipids, ceramides, acylglycerols). Here, neutral lipids will elute first before more polar and charged lipids. RPLC, conversely, separates the lipids based on hydrophobicity, that is, the carbon chain length and unsaturation (number of double bonds) of the fatty acid side chains. The application of RPLC in the second dimension is also beneficial for coupling with the mass spectrometer.

The fractionation of lipids into different classes and the chromatographic analysis of the members of each class are attractive. The combination of HILIC and RPLC has been performed offline<sup>5,6</sup> or online using a special interface for solvent evaporation.<sup>7,8</sup> In this Application Note, a fully automated multiple heart-cutting Q-TOF LC/MS analysis of complex lipid extracts with the Agilent 1290 Infinity 2D-LC solution is demonstrated.

## Experimental

### Samples and sample preparation

The lipid extraction protocol has been described in detail in reference 2. Briefly, 300  $\mu\text{L}$  of methanol was added to 50  $\mu\text{L}$  of plasma or 120  $\mu\text{L}$  of lung sputum. After vortex mixing, 1 mL of *tert*-butyl methyl ether (MTBE) was added, and the samples were incubated for one hour at room temperature. The addition of 260  $\mu\text{L}$  of water induced a phase separation, generating a lower hydrophilic and an upper lipophilic layer with a protein layer at the bottom. A 1 mL amount of the upper phase was removed and dried in a centrifugal vacuum evaporator. The dried phase was reconstituted in 100  $\mu\text{L}$  (plasma) or 40  $\mu\text{L}$  (lung sputum) of MTBE/isopropanol 50/50 (v/v), respectively.

### Instrumentation

An Agilent 1290 Infinity 2D-LC solution connected to an Agilent 6530 Q-TOF mass spectrometer was used for the experiments.

- Agilent 1290 Infinity Binary Pump (first dimension) (G4220A)
- Agilent 1290 Infinity Binary Pump (second dimension) (G4220A)
- Agilent 1290 Infinity Autosampler (G4226A)
- Agilent 1290 Infinity Thermostat (G1330A)
- Agilent 1290 Infinity Thermostatted Column Compartment (G1316C)
- Agilent 1290 Infinity valve drive (2x) (G1170A)
- Agilent 2D-LC hardware solution kit (G4236A), including loop kit for 2D-LC (option #001), capillary kit for 2D-LC (option #003), and multiple heart-cutting upgrade kit (option #007)
- Agilent 6530 Accurate-Mass Q-TOF LC/MS (G6530A)

The Jet Weaver mixer was removed in the first dimension pump to reduce the delay volume. To obtain sufficient backpressure on the first dimension separation, a calibration capillary (G1312-67500) was installed between the pump and the autosampler.

#### Software

- Agilent OpenLAB CDS ChemStation Edition (revision C.01.07) with Agilent 1290 Infinity 2D-LC Software (revision A.01.02)
- Agilent MassHunter for instrument control (revision B.05.01)
- Agilent MassHunter for data analysis (revision B.06.00)

#### Method

First dimension	HILIC
Column	Agilent RX-SIL, 1.0 × 150 mm, 3.5 μm (custom made)
Solvent A	0.1 % formic acid in acetonitrile
Solvent B	20 mM ammonium formate in acetonitrile/methanol/water, 50/20/30, v/v
Flow Rate	40 μL/min
Gradient	0 to 2 minutes: 30 to 60% B, 40 μL/min 2 to 4 minutes: 60 to 70% B, 40 μL/min 4 to 5 minutes: 70 to 100% B, 40 μL/min 5 to 12 minutes: 100% B, 40 μL/min 12 to 54 minutes: 100% B, 20 μL/min 54 to 65 minutes: 30% B, 40 μL/min
Temperature	40 °C
Second dimension	RPLC
Column	Agilent ZORBAX Eclipse Plus C18 RRHD, 2.1 × 100 mm, 1.8 μm (p/n 959758-902)
Solvent A	20 mM ammonium formate/0.1% formic acid in methanol/water, 10/90, v/v
Solvent B	20 mM ammonium formate/0.1% formic acid in acetonitrile/methanol/isopropanol, 20/30/50, v/v
Flow Rate	0.6 mL/min
Idle Flow Rate	0.2 mL/min
Gradient	0 to 6.5 minutes: 40 to 100% B 6.5 to 8.5 minutes: 100% B 8.5 to 10 minutes: 40% B
Temperature	60 °C
Loop Filling	
Time Segments	Fraction 1: 2.00 to 3.80 minutes (Loop 80 μL) Fraction 2: 3.90 to 4.80 minutes Fraction 3: 5.25 to 6.15 minutes Fraction 4: 7.80 to 8.75 minutes Fraction 5: 9.05 to 10.00 minutes
Injection	
Volume	1 μL
Sample Temperature	10 °C
Needle Wash	5 seconds flush port (MTBE/isopropanol, 25/75, v/v)
MS Detection	
Agilent JetStream Technology Source	Positive ionization, negative ionization
Drying Gas Temperature	300 °C
Drying Gas Flow	8 L/min
Nebulizer Pressure	35 psig
Sheath Gas Temperature	300 °C
Sheath Gas Flow	8 L/min
Capillary Voltage	3,500 V
Nozzle Voltage	1,000 V
Fragmentor	150 V
Centroid Data	3 spectra/s
Mass Range	m/z 200 to 1,700
Extended Dynamic Range	2 GHz
Resolution	10,000 for m/z 1,000

## Results and discussion

When lipid samples are analyzed with the described HILIC method, they elute in five to six groups in order of polarity, from neutral lipids to more polar and charged lipids. The separation of the individual lipids within each class is limited, and typically broad peaks are noted in real samples. This is shown for a plasma sample in Figure 1. The lipid classes selected in this Application Note together with the peak codes and MHC fraction are summarized in Table 1. Applying the same sample to RPLC will give a different elution pattern where the separation is based on hydrophobicity and the selectivity for the individual lipids within a class is significant (Figure 2). It is evident that the separation modes provide good orthogonality in this multidimensional LC setup.

**Table 1.** Lipids, peak codes in figures, and HILIC fractions.

Lipid Class (Abbreviation)	Code	MHC Fraction
Free fatty acids (FFA)	A	1
Monoacylglycerols (MG)	B	1
Diacylglycerols (DG)	C	1
Triacylglycerols (TG)	D	1
Cholesterol (Chol)	E	1
Cholesterol esters (CE)	F	1
Ceramides (CER)	G	1
Glycoceramides (Hex-CER)	H	1
Glyconceramides (Hex <sub>n</sub> -CER)	I	2
Phosphatidylinositols (PI)	J	2
Phosphatidylethanolamines (PE)	K	3
Glycosphingolipids (GSL)	L	3
Phosphatidylserines (PS)	M	4
Phosphatidylcholines (PC)	N	4
Sphingomyelins (SM)	O	5
Lysophospholipids (LysoPL)	P	5

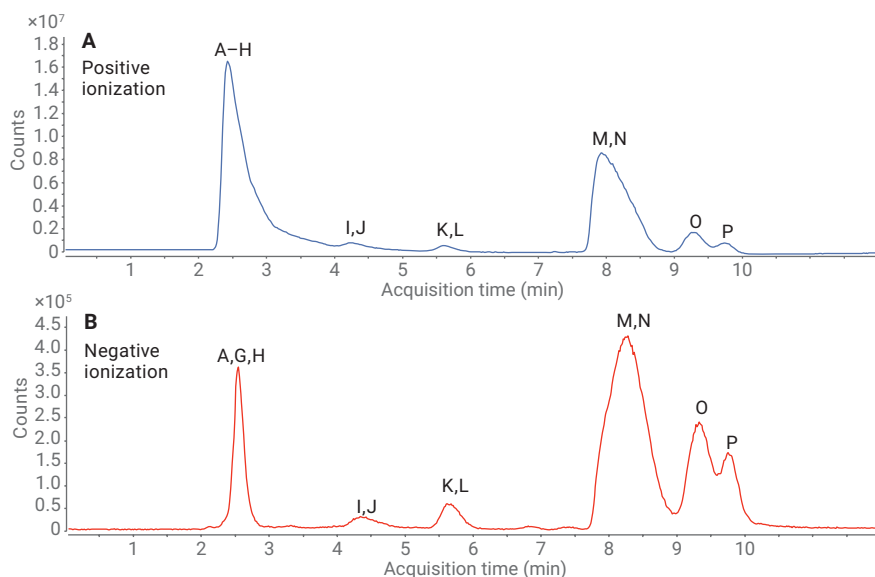


**Figure 1.** Total ion chromatogram (positive and negative ionization) for the analysis of a plasma sample with the first dimension HILIC mode.

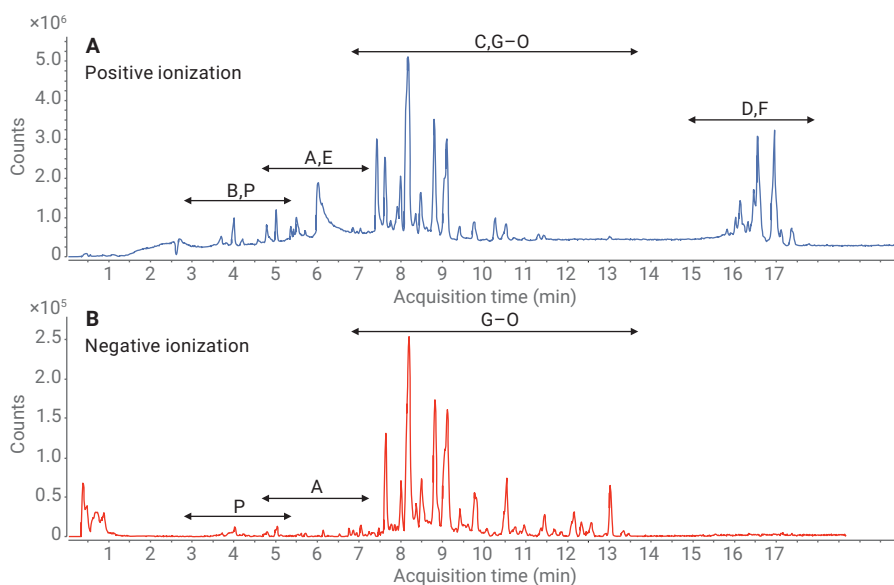


**Figure 2.** Total ion chromatogram (positive and negative ionization) for the analysis of a plasma sample with the second dimension RPLC mode (flow: 0.5 mL/min, gradient: 0 to 5 minutes: 60 to 80% B, 5 to 17 minutes: 80 to 100% B).

Using the Agilent 1290 Infinity multiple heart-cutting 2D-LC solution, a fully automated transfer of the HILIC fractions to RPLC and the subsequent analysis can be realized. The collected fractions are stored in loops installed on the 2-position/4-port duo-valve and a single multiple heart-cutting valve, and these fractions are analyzed sequentially. Filling and emptying of the loops is performed in a countercurrent fashion to reduce carryover. The order, timing, and location of storage and analysis of the fractions can be fully controlled by the 2D-LC add-on software for the Agilent OpenLAB CDS ChemStation Edition. A scheme of the valve configuration is shown in Figure 3.

The MS signals for the collected fractions of the plasma and the sputum sample can be seen in Figure 4 (for positive ionization) and Figure 5 (for negative ionization).

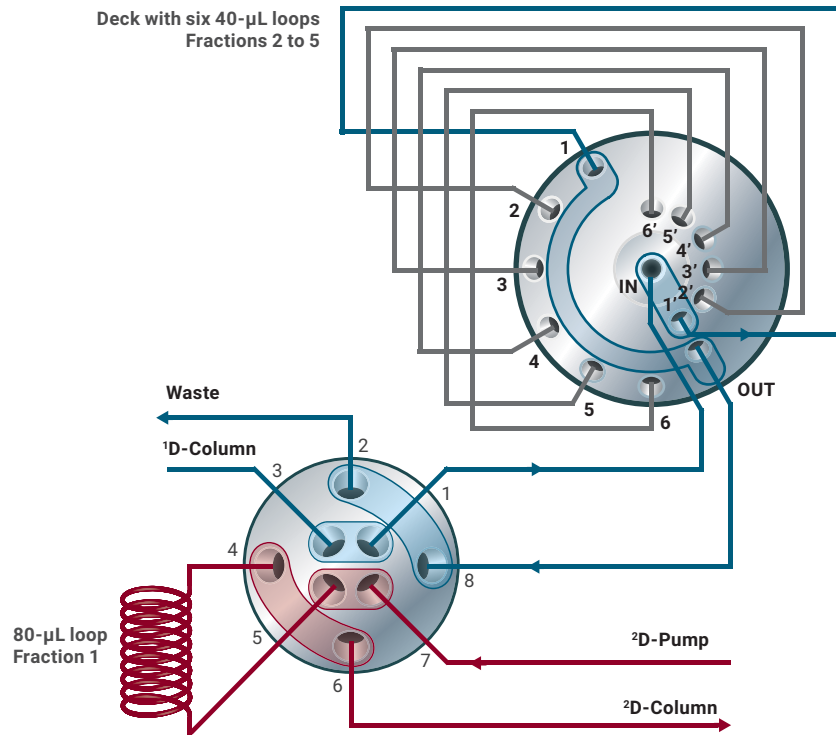


**Figure 3.** Configuration of the 2-position/4-port duo-valve for the multiple heart-cutting method. The six loops are installed on the multiple heart-cutting valve.

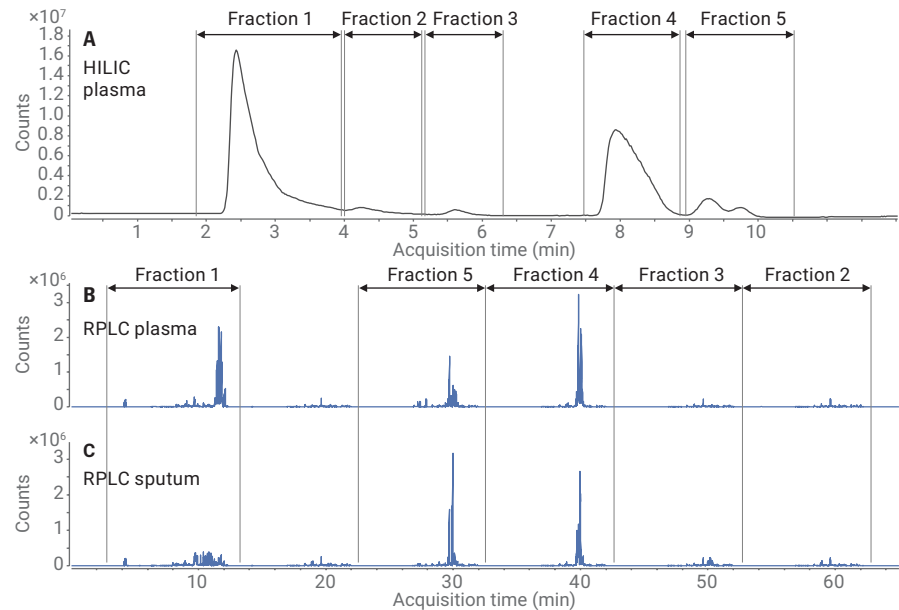


**Figure 4.** Total ion chromatogram (positive ionization) for the analysis of a plasma sample with the first dimension HILIC mode and BPC (+) of the multiple heart-cutting analyses of plasma and induced sputum.

The advantage of performing a group-type separation before separation of individual lipids is demonstrated in Figure 6. In the one-dimensional RPLC separation, there is (partial) overlap of a nearly isobaric PE and PC ( $m/z$  difference is 0.0364 Da), complicating data analysis. With the 1290 Infinity multiple heart-cutting 2D-LC solution, PCs are efficiently separated from PEs in the first dimension, and both isobaric compounds can be analyzed in separate fractions. This is a clear demonstration of the benefit of the multiple heart-cutting approach for identification and quantification of individual lipids in complex mixtures.

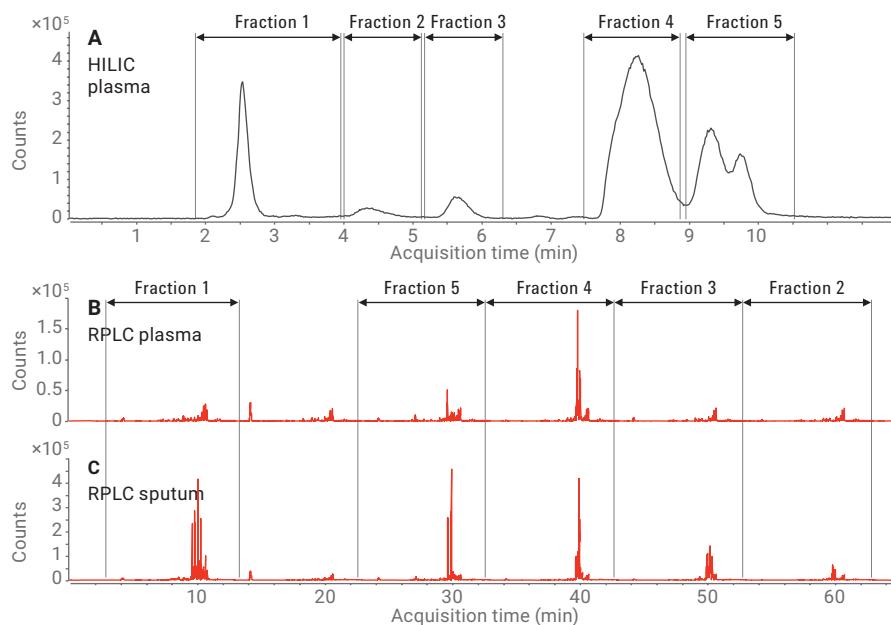


**Figure 5.** Total ion chromatogram (negative ionization) for the analysis of a plasma sample with the first dimension HILIC mode and BPC (-) of the multiple heart-cutting analyses of plasma and induced sputum.

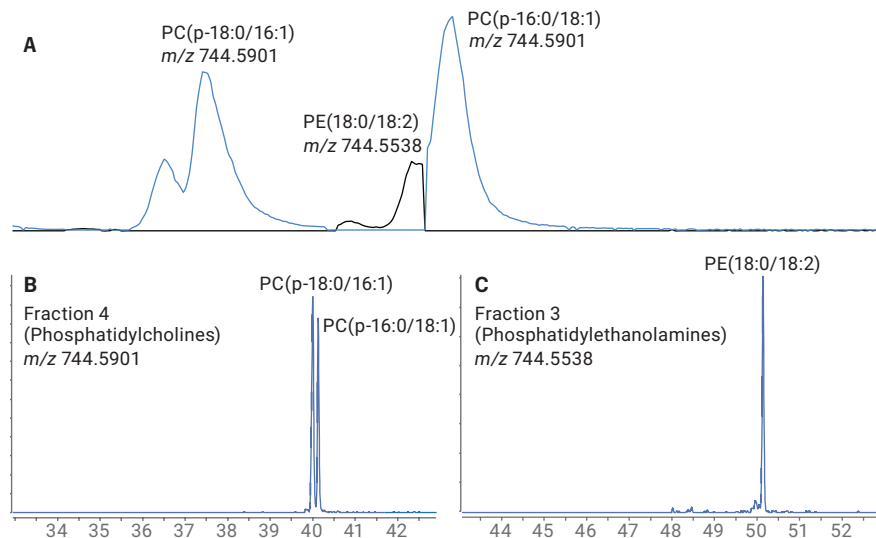
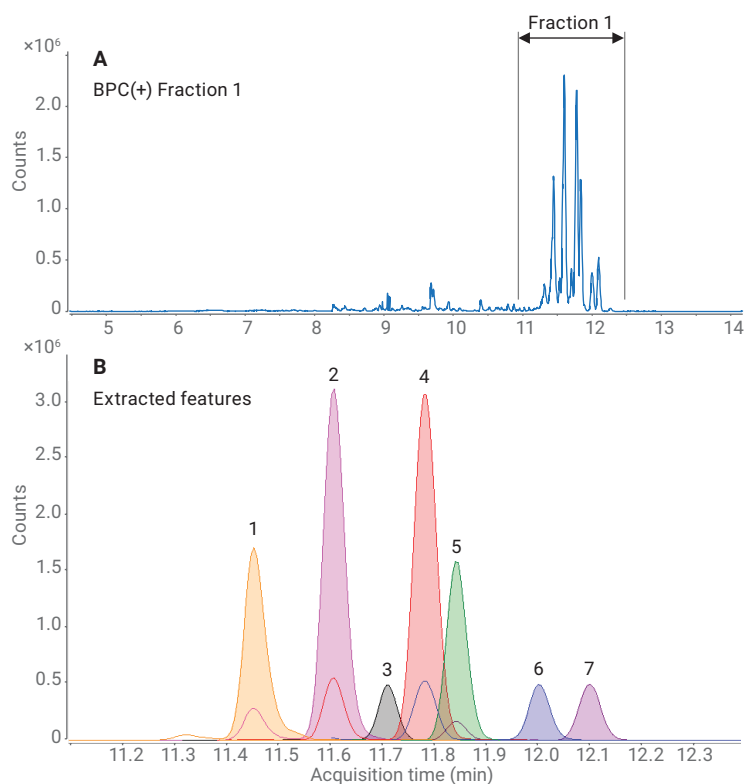


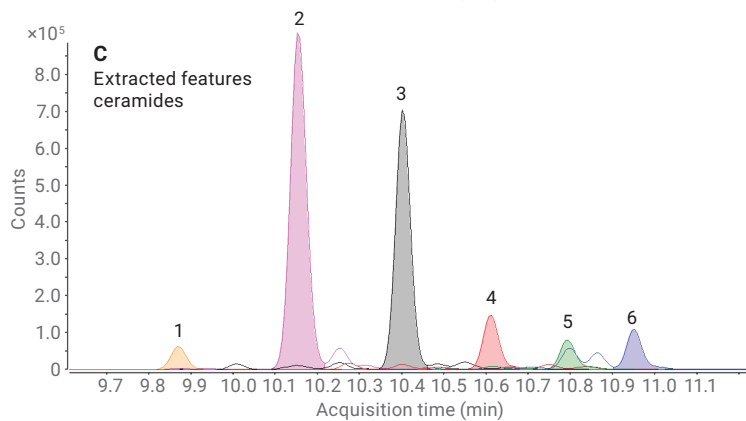
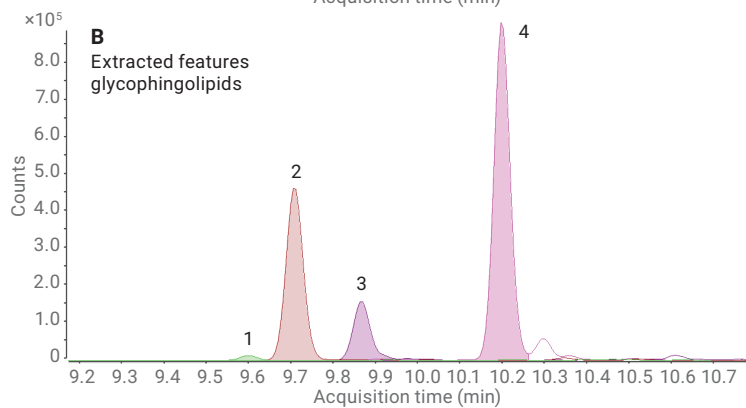
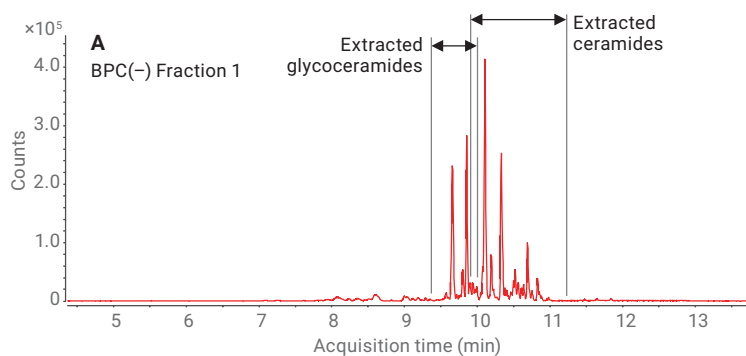
**Figure 6.** Extracted ion chromatogram (positive ionization) for selected PEs and PCs in a plasma sample. (A) shows the one-dimensional RPLC separation, (B) traces show the results for the multiple heart-cutting analyses where PEs and PCs are separated in the first dimension HILIC separation.

To further illustrate the performance of multiple heart-cutting 2D-LC and the usefulness of this technique in lipidome studies, some specific structure elucidations are presented in Figure 7 through Figure 12. The nomenclature proposed by the International Lipid Classification and Nomenclature Committee (ILCNC) is used.<sup>9</sup>



Feature	Formula	$t_R$ (min)	$m/z$	Identity
1	$C_{55}H_{101}O_6N$	11.45	871.7629	TG(52:4)NH <sub>3</sub>
2	$C_{55}H_{100}O_6N$	11.61	873.7786	TG(52:3)NH <sub>3</sub>
3	$C_{47}H_{79}NO_2$	11.71	689.6111	CE(20:4)NH <sub>3</sub>
4	$C_{55}H_{105}O_6N$	11.78	875.7942	TG(52:2)NH <sub>3</sub>
5	$C_{45}H_{79}NO_2$	11.84	665.6111	CE(18:2)NH <sub>3</sub>
6	$C_{55}H_{107}O_6N$	12	877.8099	TG(52:1)NH <sub>3</sub>
7	$C_{45}H_{81}NO_2$	12.1	667.6267	CE(18:1)NH <sub>3</sub>

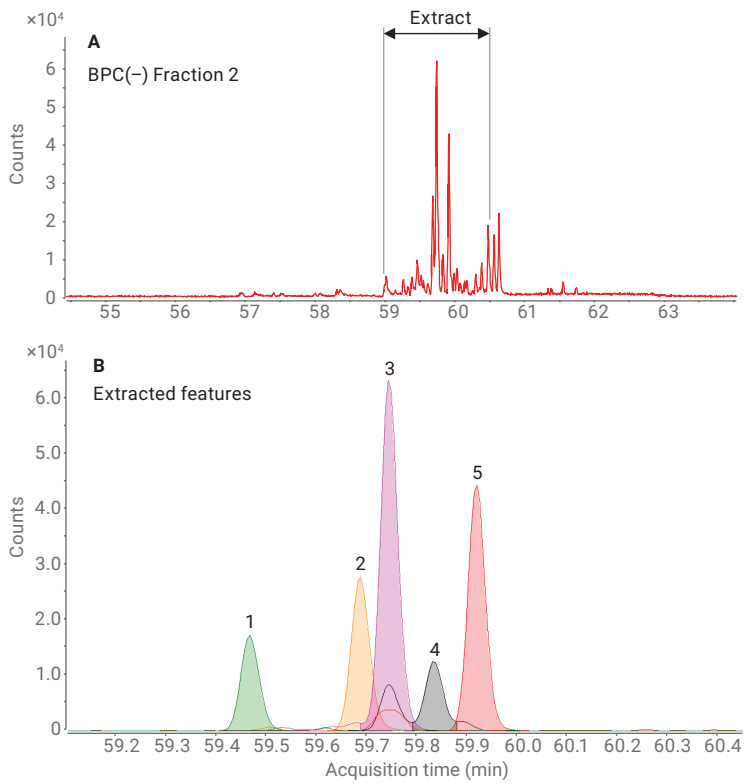
**Figure 7.** Fraction 1, positive ionization, triglycerides, and cholesterol esters in plasma. TG and CE represent the most apolar lipids. Both groups are detected as ammonia adducts in the positive ESI mode.



Feature (Glycosphingolipids)	Formula	$t_R$ (min)	$m/z$	Identity
1	$C_{52}H_{97}NO_{18}$	9.56	1023.670565	HexHexHexCER(NS)(34)
2	$C_{46}H_{67}NO_{13}$	9.66	861.6177417	HexHexCER(NS)(34)
3	$C_{40}H_{77}NO_8$	9.81	699.5649183	HexCER(NS)(34)
4	$C_{34}H_{67}NO_3$	10.11	537.512094	CER(NS)(34)

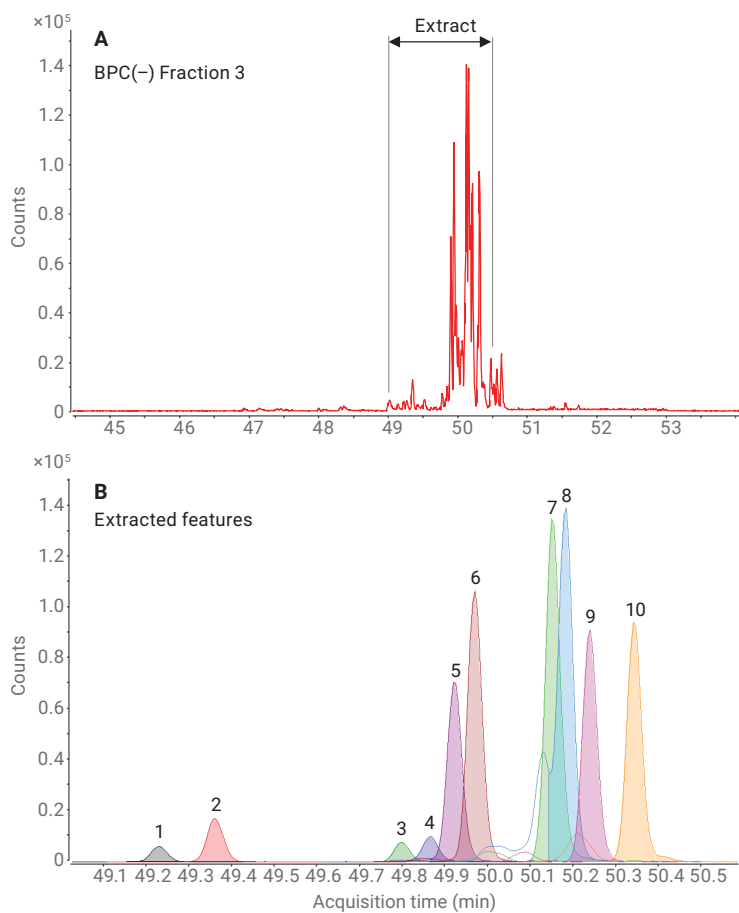
Feature (Ceramides)	Formula	$t_R$ (min)	$m/z$	Identity
1	$C_{32}H_{63}NO_3$	9.85	509.480794	CER(NS)(32)
2	$C_{34}H_{67}NO_3$	10.11	537.512094	CER(NS)(34)
3	$C_{36}H_{71}NO_3$	10.33	565.543394	CER(NS)(36)
4	$C_{38}H_{75}NO_3$	10.53	593.574694	CER(NS)(38)
5	$C_{40}H_{79}NO_3$	10.69	621.605994	CER(NS)(40)
6	$C_{42}H_{83}NO_3$	10.83	649.637294	CER(NS)(42)

**Figure 8.** Fraction 1, negative ionization, sphingolipids in sputum. Ceramides and smaller glycosphingolipids are preferentially detected in negative ESI mode. Elution order is based on the attached sugar moiety and the fatty acid side chain.



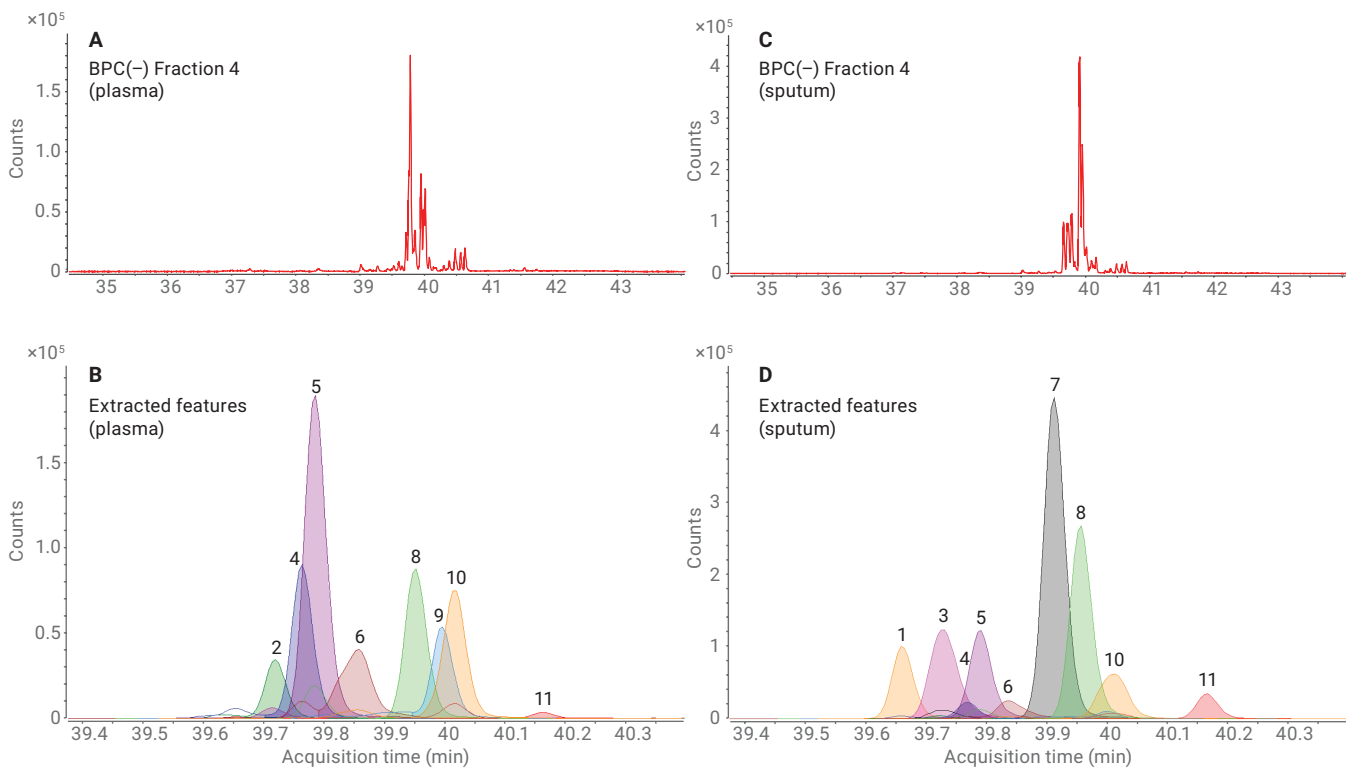
Feature	Formula	$t_R$ (min)	$m/z$	Identity
1	$C_{52}H_{97}NO_{18}$	59.46	1023.671	HexHexHexCer(NS)(34)
2	$C_{43}H_{81}O_{13}P$	59.68	836.5415	PI(18:1/16:0)
3	$C_{47}H_{83}O_{13}P$	59.75	886.5571	PI(18:0/20:4)
4	$C_{47}H_{85}O_{13}P$	59.85	888.5728	PI(18:0/20:3)
5	$C_{45}H_{85}O_{13}P$	59.94	864.5728	PI(18:1/18:0)

**Figure 9.** Fraction 2, negative ionization, phosphatidylinositols in sputum. Phosphatidylinositols encompass approximately 5% of detected glycerophospholipids in sputum. HexHexHexCer(NS)(34) is present in both Fractions 1 and 2.



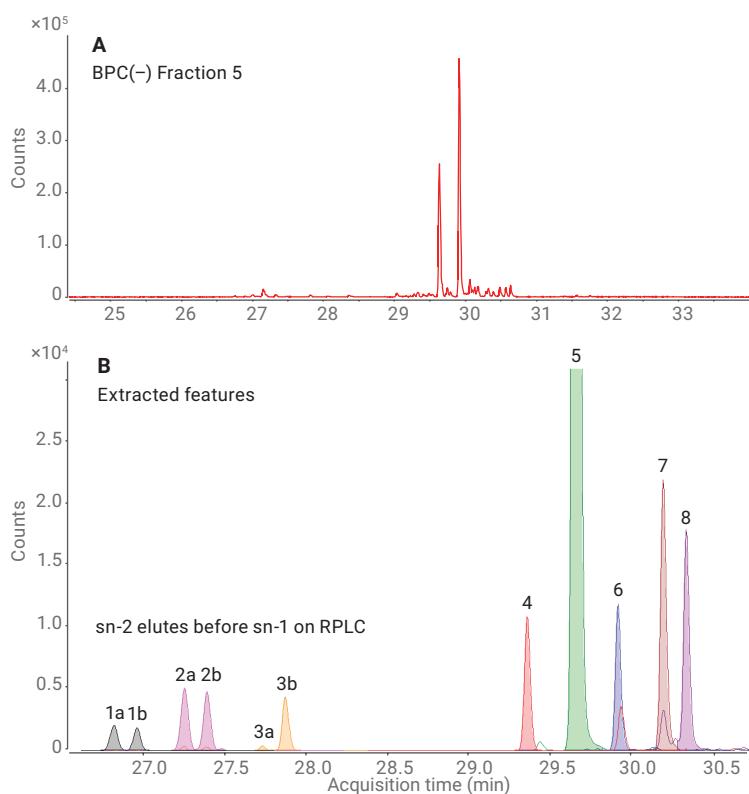
Feature	Formula	$t_r$ (min)	$m/z$	Identity
1	$C_{57}H_{104}N_2O_{21}$	49.22	1152.713	NeuAcHexHexCER(d18:1/16:0)
2	$C_{60}H_{110}N_2O_{23}$	49.35	1226.75	HexNAcHexHexHexCER(d18:1/16:0)
3	$C_{37}H_{72}NO_8P$	49.78	689.4996	PE(32:1)
4	$C_{39}H_{74}NO_8P$	49.85	715.5152	PE(16:0/18:2)
5	$C_{43}H_{74}NO_7P$	49.9	747.5203	PE(p16:0/22:6)
6	$C_{41}H_{74}NO_7P$	49.95	723.5203	PE(p16:0/20:4)
7	$C_{39}H_{76}NO_7P$	50.13	701.5359	PE(p16:0/18:1)
8	$C_{43}H_{78}NO_7P$	50.16	751.5516	PE(p18:0/20:4)
9	$C_{41}H_{80}NO_7P$	50.31	729.5672	PE(p18:0/18:1)
10	$C_{41}H_{80}NO_8P$	50.22	745.5622	PE(18:0/18:1)

**Figure 10.** Fraction 3, negative ionization, phosphatidylethanolamines, and glycosphingolipids in sputum. Plasmalogen phosphatidylethanolamines (PEp) are highly abundant in lung sputum. Complex glycosphingolipids containing N-acetylneuraminic acid (Neu5Ac) elute in this fraction.



Feature	Formula	$t_r$ (min)	$m/z$	Identity
1	$C_{39}H_{78}NO_{10}P$	39.66	751.5363	PC(16:0/14:0)formate
2	$C_{47}H_{82}NO_{10}P$	39.72	851.5676	PC(16:0/22:6)formate
3	$C_{41}H_{80}NO_{10}P$	39.73	777.552	PC(16:0/16:1)formate
4	$C_{45}H_{82}NO_{10}P$	39.76	827.5676	PC(16:0/20:4)formate
5	$C_{43}H_{82}NO_{10}P$	39.78	803.5676	PC(34:2)formate
6	$C_{45}H_{84}NO_{10}P$	39.86	829.5833	PC(18:1/18:2)formate
7	$C_{41}H_{82}NO_{10}P$	39.91	779.5676	PC(16:0/16:0)formate
8	$C_{43}H_{84}NO_{10}P$	39.96	805.5833	PC(16:0/18:1)formate
9	$C_{47}H_{86}NO_{10}P$	39.99	855.5989	PC(18:0/20:4)formate
10	$C_{45}H_{86}NO_{10}P$	40.02	831.5989	PC(36:2)formate
11	$C_{45}H_{88}NO_{10}P$	40.17	833.6146	PC(18:0/18:1)formate

**Figure 11.** Fraction 4, negative ionization, phosphatidylcholines (PC) in sputum and plasma. Phosphatidylcholines are highly abundant in both samples. Both samples show different PC patterns. PCs are detected as formate adducts in negative ESI mode.



Feature	Formula	$t_R$ (min)	$m/z$	Identity
1a	$C_{27}H_{52}NO_8P$	26.75	565.33797	PC(0:0/18:2)formate
1b	$C_{27}H_{52}NO_8P$	26.89	565.33797	PC(18:2/0:0)formate
2a	$C_{27}H_{54}NO_8P$	27.19	567.35362	PC(0:0/18:1)formate
2b	$C_{27}H_{54}NO_8P$	27.33	567.35362	PC(18:1/0:0)formate
3a	$C_{27}H_{56}NO_8P$	27.68	569.36927	PC(0:0/18:0)formate
3b	$C_{27}H_{56}NO_8P$	27.82	569.36927	PC(18:0/0:0)formate
4	$C_{38}H_{77}N_2O_8P$	29.33	720.5418	SM(d18:1/14:0)formate
5	$C_{40}H_{81}N_2O_8P$	29.63	748.5731	SM(d18:1/16:0)formate
6	$C_{42}H_{85}N_2O_8P$	29.9	776.6044	SM(d18:1/18:0)formate
7	$C_{48}H_{95}N_2O_8P$	30.32	858.6826	SM(d18:1/24:1)formate
8	$C_{48}H_{93}N_2O_8P$	30.18	856.667	SM(d18:1/24:2)formate

**Figure 12.** Fraction 5, negative ionization, lysophosphatidylcholines and sphingomyelins in sputum. Sn-2 lysophospholipids elute before sn-1 lysophospholipids in RPLC. Both lipid subclasses are detected as formate adducts in negative ESI mode.

## Conclusion

The Agilent 1290 Infinity 2D-LC solution was used for fully automated multiple-heart-cutting analyses of the blood plasma and induced sputum lipidome. The lipids were fractionated in HILIC mode, and the fractions were then transferred to and analyzed with RPLC. Detection with the Agilent 6530 Accurate-Mass Q-TOF LC/MS System facilitated identification of the individual lipids in each fraction. Selected data clearly demonstrate the power of the system in lipidomics and might be extended to other metabolomic applications.

## References

1. Sandra, K.; Sandra, P. Lipidomics From an Analytical Perspective, *Curr. Opin. Chem. Biol.* **2013**, *17*, 847–853.
2. Sandra, K.; *et al.* Comprehensive Blood Plasma Lipidomics by Liquid Chromatography/Quadrupole Time-of-Flight Mass Spectrometry, *J. Chromatogr. A* **2010**, *1217*, 4087–4099.
3. Telenga, E.; *et al.* Untargeted Lipidomic Analysis in Chronic Obstructive Pulmonary Disease, *Am. J. Respir. Crit. Care Med.* **2014**, *190*, 155–164.
4. Francois, I.; Sandra, K.; Sandra, P. Comprehensive Liquid Chromatography: Fundamental Aspects and Practical Considerations – a Review, *Anal. Chim. Acta.* **2009**, *64*, 14–31.
5. Lisa, M.; Cifkova, E.; Holcapek, M. Lipidomic Profiling of Biological Tissues Using Off-Line Two-Dimensional High-Performance Liquid Chromatography-Mass Spectrometry, *J. Chromatogr. A* **2011**, *1218*, 5146–5156.
6. Cifkova, E.; Holcapek, M.; Lisa, M. Nontargeted Lipidomic Characterization of Porcine Organs Using Hydrophilic Interaction Liquid Chromatography and Offline Two-Dimensional Liquid Chromatography-Electrospray Ionization Mass Spectrometry, *Lipids* **2013**, *48*, 915–928.
7. Nie, H.; *et al.* Lipid Profiling of Rat Peritoneal Surface Layers by Normal- and Reversed-Phase 2D LC QTOF-MS, *J. Lipid Res.* **2010**, *51*, 2833–2844.
8. Li, M.; *et al.* Lipid Profiling of Human Plasma from Peritoneal Dialysis Patients Using an Improved 2D (NP/RP) LC-QTOF MS Method, *Anal. Bioanal. Chem.* **2013**, *405*, 6629–6638.
9. Fahy, E.; *et al.* Lipid Classification, Structures and Tools, *Biochim. Biophys. Acta.* **2011**, *1811*, 637–647.

[www.agilent.com/chem](http://www.agilent.com/chem)

**For Research Use Only. Not for use in diagnostic procedures.**

This information is subject to change without notice.

© Agilent Technologies, Inc. 2015, 2019  
Printed in the USA, May 28, 2019  
5991-5532EN

